IJIREEICE ISSN (O) 2321-2004, ISSN (P) 2321-5526

International Journal of Innovative Research in Electrical, Electronics, Instrumentation and Control Engineering

Impact Factor 8.021 ⁜ Peer-reviewed & Refereed journal ⁜ Vol. 12, Issue 11, November 2024

DOI: 10.17148/IJIREEICE.2024.121101

Machine Learning Technique for Faults Identification in Microgrid

Sri R. Kolla[1], Peter Onwonga[2]

Professor, Electronics and Computer Engineering Technology, Bowling Green State University, Bowling Green, USA[1]

Student, Electronics and Computer Engineering Technology, Bowling Green State University, Bowling Green, USA[2]

Abstract: In this paper a machine learning technique-based method is presented for identifying faults in a microgrid. The machine learning method considered is multilayer neural network. The microgrid model includes renewable energy sources such as solar photovoltaic and wind generator. Both normal and fault situations for the microgrid are simulated when operating in grid-connected and islanded modes. The fault conditions include various faults experienced on a power distribution line. The fault currents and voltages are used for training a neural network with Levenberg-Marquardt method. The trained neural network is effective in identifying and classifying faults using trained and untrained data for both grid-connected and islanded modes of operation.

Keywords: Machine Learning, Microgrid, Neural Network, Protective Relaying, Fault Detection.

I. INTRODUCTION

The traditional electric power grid is struggling with operational constraints. An approach to overcome these challenges is to integrate renewable energy sources such as solar and wind. The integration of renewable and distributed energy sources has resulted in the development of microgrids by utilizing power electronics, control and protection devices that can operate in both grid-connected and islanded modes [1]. One of the challenges with the microgrid is designing a reliable protection system that can work in both modes of operation [2]. The traditional protection schemes may not work successfully for the microgrid because of low fault currents in islanded mode and bi-directional current flows due to distributed sources [3-8].

At present, several techniques are implemented for the microgrid fault diagnosis in digital relays that include adaptive protection [9,10], differential protection [11,12], voltage-based protection [13], current-based protection [14-16], impedance-based (distance) protection [17,18], differential energy-based protection [19], multiagent protection [20], and transient-based protection [21] schemes. Artificial Intelligence (AI) techniques are also explored for the microgrid protection in recent years by some researchers [22]. These include Artificial Neural Networks (ANN) [23-25], support vector machines and other classification methods [26-28], fuzzy logic [29] and data mining [30,31]. However, the method in [25] applied ANN to identify faults in only islanded mode operation of the microgrid. This paper extends these concepts and applies the neural network to identify faults in both grid-connected and islanded mode of operation of the microgrid.

This paper presents a Machine Learning (ML) technique-based method to identify faults in the microgrid that operates in both grid-connected and islanded modes. An introductory review of ML and neural networks is presented in Section II. The microgrid operation in grid-connected and islanded modes, and different types of faults experienced by it are then explained in Section III. Both the normal operation and fault situations for the microgrid are simulated in Simulink [32] when operating in both modes for a microgrid test system. Details of these simulations are given in Section III. Application of ML to the microgrid protection is outlined in Section IV. MATLAB [32] is used for training the neural network with the simulated data. The trained neural network is successful in identifying faults using trained and untrained data for both grid-connected and islanded modes of operations. These test results are discussed in Section IV. Concluding remarks are offered in Section V.

II. MACHINE LEARNING

Machine learning is a branch of artificial intelligence that enables machines to perform tasks by learning from data [33]. There are several machine learning techniques such as neural networks and support vector machines. The neural networks are popular because of their capability to recognize patterns in complex and large data. The machine learning area has

IJIREEICE ISSN (O) 2321-2004, ISSN (P) 2321-5526

International Journal of Innovative Research in Electrical, Electronics, Instrumentation and Control Engineering

Impact Factor 8.021 ⁜ Peer-reviewed & Refereed journal ⁜ Vol. 12, Issue 11, November 2024

DOI: 10.17148/IJIREEICE.2024.121101

received significant attention from researchers in recent years because of deep learning techniques that showed promising real-life applications in vision and autonomous vehicles.

Neural networks have perceptrons (neurons) in layers that have weighted connections to successive layers [33]. These neural networks have input layer, hidden layers, and output layer as shown in Figure 1. A mathematical model of a perceptron (neuron) is given by Equation (1).

$$o = f(\sum_{j=1}^{m} w_j i_j + c) \quad (1)$$

A weighted (w) sum of inputs (i) with a bias (c) is calculated using Equation (1) and sent to an activation function. The popular activation functions are linear, sign, step and sigmoid functions. Equation (2) is the sigmoid function used in several applications.

$$f(x) = \frac{1}{1+e^{-x}} \quad (2)$$

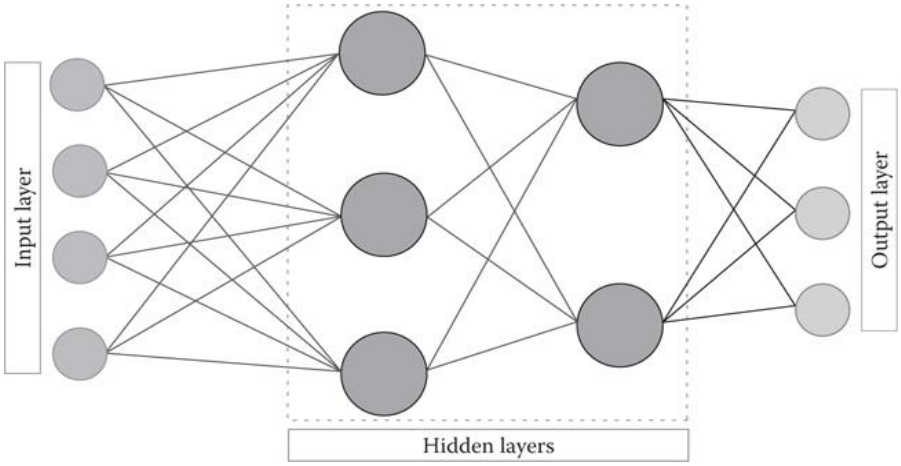

Figure 1. Neural network

The number of neurons in the input and the output layers is determined by the input and output data sizes. The number of hidden layers and neurons in these is usually determined by heuristic methods [33]. For a neural network, there is an optimum number of hidden layers and neurons in them, above which may result in overfitting results. Learning methods are used to train and adjust the weights of the neural network to recognize a pattern of the given data. The Levenberg-Marquardt and backpropagation are some of the training methods. The Levenberg-Marquardt method for adjusting weights, w, at p-th iteration is given in Equation (3):

$$w(p+1) = w(p) - [\, J(p)^T J(p) + \mu I \,]^{-1} J(p)^T e(p) \quad (3)$$

where μ is the damping factor adjusted at every iteration until the sum of the square error is reduced. J is the Jacobian matrix with first derivatives of the errors (e).

The neural network-based machine learning method for microgrid faults identification uses the following steps: i) selection of inputs and outputs, ii) selection of neural network structure, and iii) training and testing of the neural network. The RMS values of three-phase currents and voltages are selected as inputs. The outputs denote no-fault and various fault conditions. The output is 1 if that condition occurs, otherwise the output is 0. Figure 2 shows these inputs and outputs selection of the neural network. The network contains six input neurons and five output neurons. The input neurons use RMS values of three-phase currents and voltages. The five output neurons corresponding to one case of normal operation or no-fault and four categories of shunt-faults [34]. The hidden layers number and the neurons in each layer is selected to assist the training.

IJIREEICE ISSN (O) 2321-2004, ISSN (P) 2321-5526

International Journal of Innovative Research in Electrical, Electronics, Instrumentation and Control Engineering

Impact Factor 8.021 ⁜ Peer-reviewed & Refereed journal ⁜ Vol. 12, Issue 11, November 2024

DOI: 10.17148/IJIREEICE.2024.121101

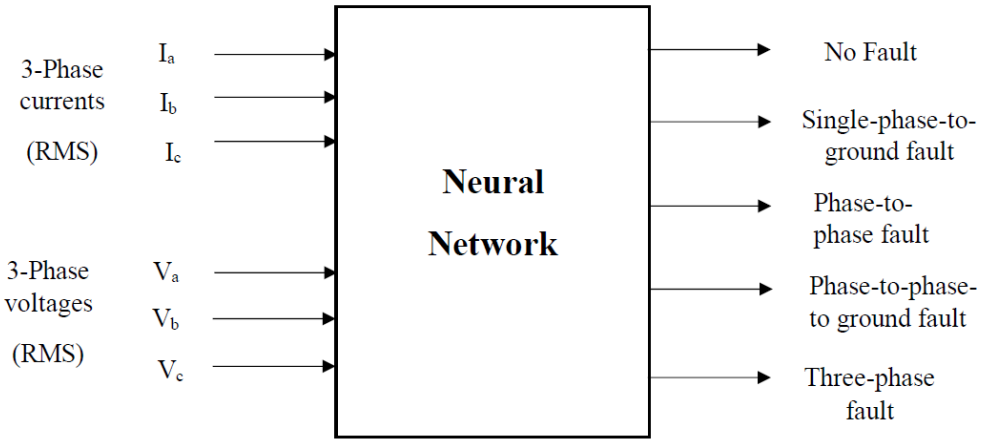

Figure 2. Inputs and outputs of neural network for microgrid faults identification

III. MICROGRID TEST SYSTEM

In this paper a modified IEEE 13 bus test feeder is used to integrate microgrid sources and loads shown in Figure 3 [25]. Some of the characteristics of the feeder are given in [35] and it operates at 4.16 kV. The following renewable and other energy sources are connected to this feeder and are used in Simulink [36] simulation:

1. The solar Photo Voltaic (PV) system model used is rated at 250 V, 250 KW. The generated voltage is stepped to 4.16 kV. It connects to the test feeder at bus 635 with a 0.15km, 4.16 kV line.
2. The wind generator model used contain the wind turbine, Doubly Fed Induction Generator (DFIG), AC/DC/AC converter, and a control system. The wind generator is rated at 575 V and 1.5MW. The generated voltage is stepped to 4.16 kV. It connects to the test feeder at bus 682 with a 0.24km, 4.16 kV line.
3. The synchronous generator model is used to study the diesel generator performance. The diesel engine is modeled by a transfer function. The synchronous generator is modeled in the usual DQ reference frame. The system is rated at 2.4 kV and 3.125 MVA. This generated voltage is stepped to 4.16 kV. It is then connected to the test feeder at bus 680 with a 0.2km 4.16 kV line.

The system has a total load of about 3 MVA comprising real and reactive powers. The main loads are connected at buses 632, 634, 671, 675 and 692.

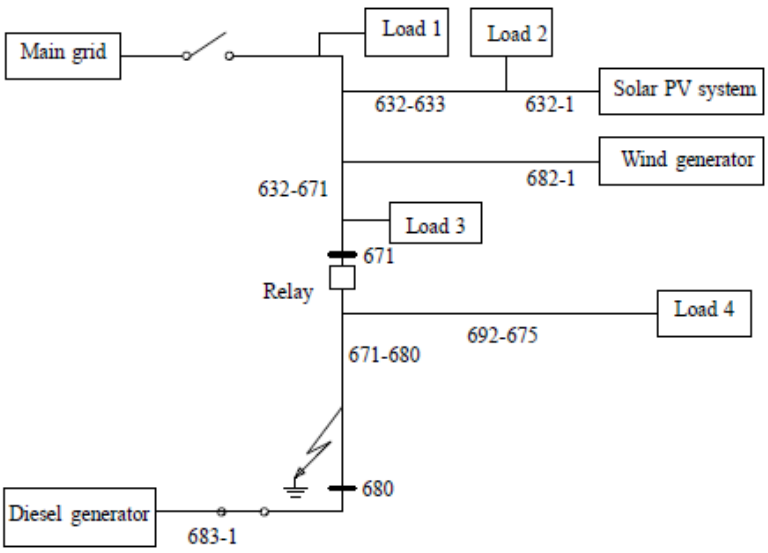

Figure 3. Microgrid test system

IJIREEICE ISSN (O) 2321-2004, ISSN (P) 2321-5526

International Journal of Innovative Research in Electrical, Electronics, Instrumentation and Control Engineering

Impact Factor 8.021 ⁜ Peer-reviewed & Refereed journal ⁜ Vol. 12, Issue 11, November 2024

DOI: 10.17148/IJIREEICE.2024.121101

During the islanded and the grid-connected mode operations of the microgrid, the wind generator and solar PV system run simultaneously supplying power within their installed capacity. The main grid provides the remaining load power that is not supplied by renewable energy sources in the grid-connected mode. In grid-connected mode the diesel generator is off-line but in the islanded mode supplies the load not met by the wind generator and the solar PV system.

The simulation of the modeled microgrid is done with a computation step size of $5x10^{-8}$ sec. However, for this application, only 36 samples per 60 Hz cycle are used. In this paper the total simulation for each fault/normal operation case is done for 0.09 seconds representing 5.4 cycles of operation. This results in 195 samples for 5.4 cycles of the simulation.

A. FAULTS SIMULATION ON MICROGRID

Faults are simulated on the distribution line connecting buses 671 and 680 of the system shown in Figure 3. Data is collected at bus 671 representing the relay location. The faults are simulated at 10% distance increments from the relay location to the other end of the line representing 100%. These faults consist of four types: single-phase-to-ground, phase-to-phase-to-ground, phase-to-phase and three phase-to-ground faults [37]. The data corresponding to these faults are collected and used for training the neural network. Faults are also created at other distances, for instance, 25% and 55%, to test the trained neural network. Both grid-connected mode and islanded mode of operations are considered, and the data for these are given in the following sub-sections.

The collected data consists of instantaneous values. The fundamental frequency RMS values are computed using these with one cycle of data samples. The Discrete Fourier Transform (DFT) given in Equation (4) [37] is used:

$$X = \frac{2}{N}\sum_{k=0}^{N-1} x_k \, e^{-j2\pi k/N} \qquad (4)$$

where, x_k is the sample value of the signal, X is RMS value and N is the number of samples per cycle. As indicated before, N=36 samples per cycle are used. These three-phase current and voltage RMS values are used for training and testing the proposed neural network faults identification method.

1. Grid-connected mode:

Figure 4 shows three-phase currents and voltages at the relay location for phase-to-ground fault at 50% distance of the line from the relay location. These currents and voltages show transients once the fault is applied after 2.4 cycles. A three-cycle fault data is shown in these figures. These transients include high-frequency components and decaying DC components. Similar characteristics are observed for other fault distances data.

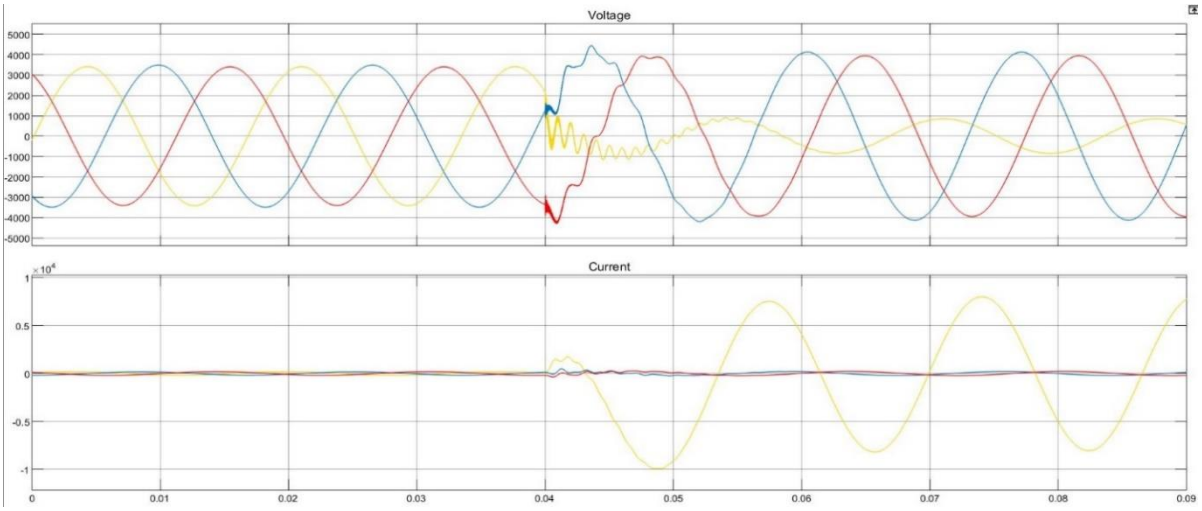

Figure 4. Currents and voltages at relay location for phase-to-ground fault in grid-connected mode

The DFT method described before is used to calculate the RMS values from the sampled instantaneous currents and voltages. For the three phase voltages and currents shown in Figure 6, the RMS values of voltages are shown in Figure 5, while Figure 6 shows the RMS values for three-phase currents. The first RMS value sample calculations in these figures use the previous 36 samples (one cycle) of instantaneous values. The plot shows the remaining 4.4 cycles of RMS

IJIREEICE ISSN (O) 2321-2004, ISSN (P) 2321-5526

International Journal of Innovative Research in Electrical, Electronics, Instrumentation and Control Engineering

Impact Factor 8.021 ⁜ Peer-reviewed & Refereed journal ⁜ Vol. 12, Issue 11, November 2024

DOI: 10.17148/IJIREEICE.2024.121101

values representing 159 samples. These currents and voltages at the relay location are used for training and testing of the neural network.

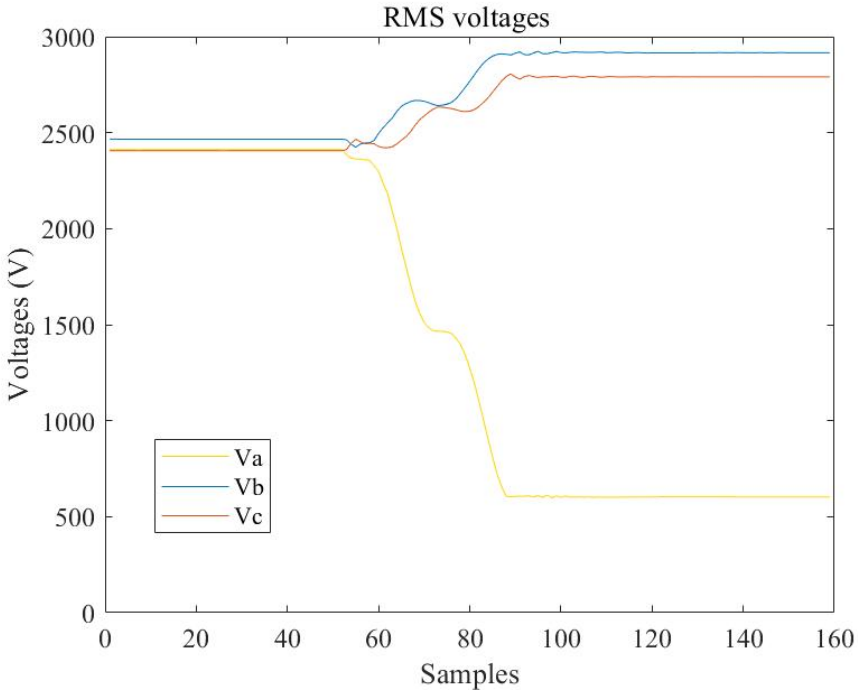

Figure 5. RMS values of voltages at relay location for phase-to-ground fault in grid-connected mode

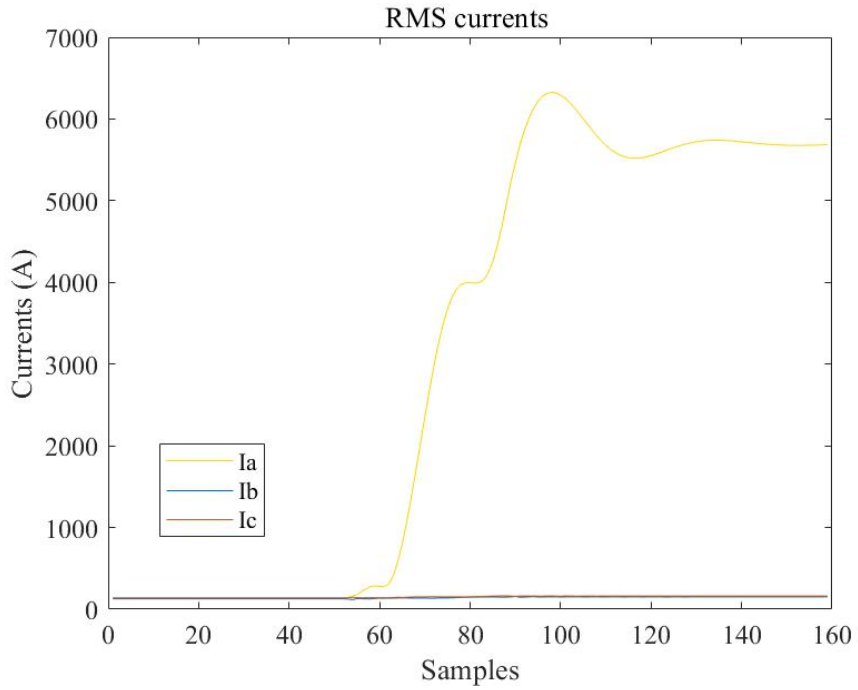

Figure 6. RMS values of currents at relay location for phase-to-ground fault in grid-connected mode

IJIREEICE ISSN (O) 2321-2004, ISSN (P) 2321-5526

International Journal of Innovative Research in Electrical, Electronics, Instrumentation and Control Engineering

Impact Factor 8.021 ⁜ Peer-reviewed & Refereed journal ⁜ Vol. 12, Issue 11, November 2024

DOI: 10.17148/IJIREEICE.2024.121101

2. ISLANDED MODE:

Figure 7 shows three-phase currents and voltages at the relay location for single-phase-to-ground fault at 50% distance of the line from the relay location [25]. These currents and voltages show transients consisting of high-frequency components and decaying DC components after fault is applied. It also shows some initial transients from simulation. Similar characteristics are observed for other fault distances data. It can also be observed that the steady state fault currents for islanded mode are lower than the grid-connected mode. This suggests that the traditional overcurrent relays may not perform appropriately with the same settings for both modes of operation. This transpires the need to explore machine learning techniques for protection of microgrids to work for both modes of operation. These currents and voltages at the relay location are used for training and testing of the neural network.

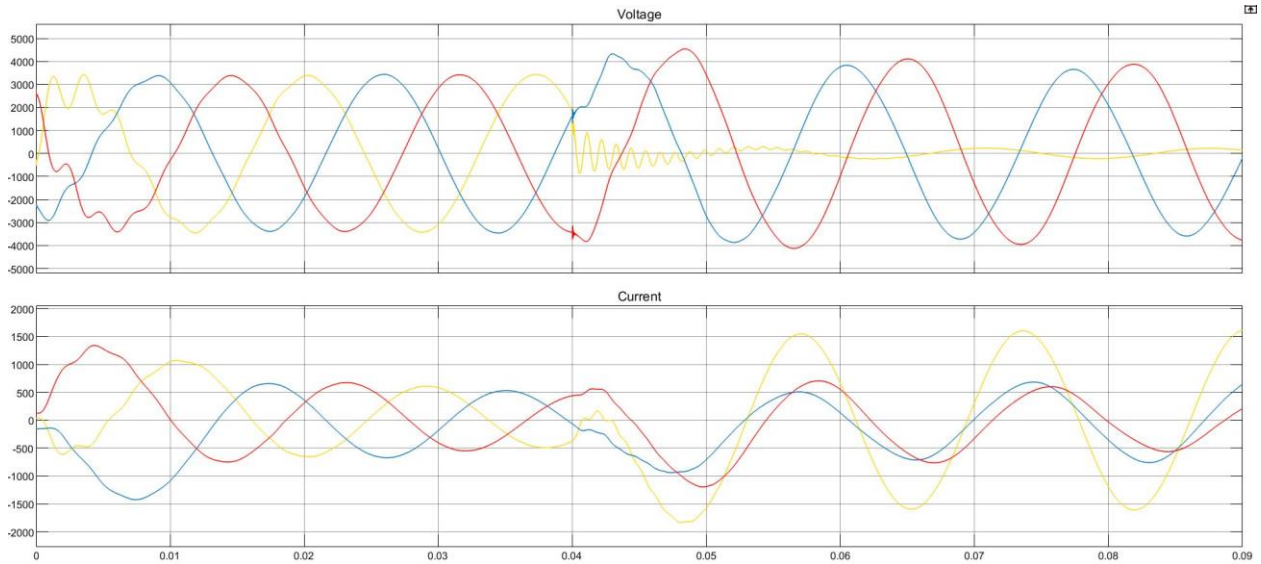

Figure 7. Currents and voltages at relay location for phase-to-ground fault in islanded mode

IV. TRAINING AND TESTING RESULTS FOR DETECTING MICROGRID FAULTS

Simulated data representing various faults from the microgrid test system described in the previous section are used for training and testing of the neural network-based faults identification method. These results are presented in this section.

A. NEURAL NETWORK TRAINING RESULTS

The RMS values of voltages and currents are used to train the neural network. The data corresponding to different faults created at 10% increment distances from the relay location of the line, in addition to no fault case, are arranged in the required format as input for the neural network training in MATLAB. The output for training is also created in the MATLAB. Examples of partial input and output files data are shown in Tables I and II. In Table I, the voltages are divided by 1,000 and currents are divided by 10,000 to scale the data for training.

Table I Inputs for neural network training.

Va	Vb	Vc	Ia	Ib	Ic
2.4117	2.4666	2.4061	0.0138	0.0128	0.0139
0.6029	2.916	2.7909	0.5683	0.0151	0.0161
2.3902	1.2768	1.3003	0.0137	0.7363	0.7235
2.8927	0.5563	0.5824	0.0166	0.7823	0.7376
0.5344	0.543	0.5393	0.9618	0.9603	0.8276

IJIREEICE ISSN (O) 2321-2004, ISSN (P) 2321-5526

International Journal of Innovative Research in Electrical, Electronics, Instrumentation and Control Engineering

Impact Factor 8.021 ⁜ Peer-reviewed & Refereed journal ⁜ Vol. 12, Issue 11, November 2024

DOI: 10.17148/IJIREEICE.2024.121101

Table II Outputs for ANN training.

NF	PG	PP	PPG	3PG
1	0	0	0	0
0	1	0	0	0
0	0	1	0	0
0	0	0	1	0
0	0	0	0	1

For the combined grid-connected and islanded mode data, the total trained data consisted of 4,788 samples from grid-connected operation and 4,446 samples from islanded operation. Two hidden layer neural network with nine neurons in the first hidden layer and eight neurons in the second hidden layer shown in Figure 8 is used. The network is trained using the Levenberg Marquardt method. The network trained in 53 iterations with error histogram shown in Figure 9.

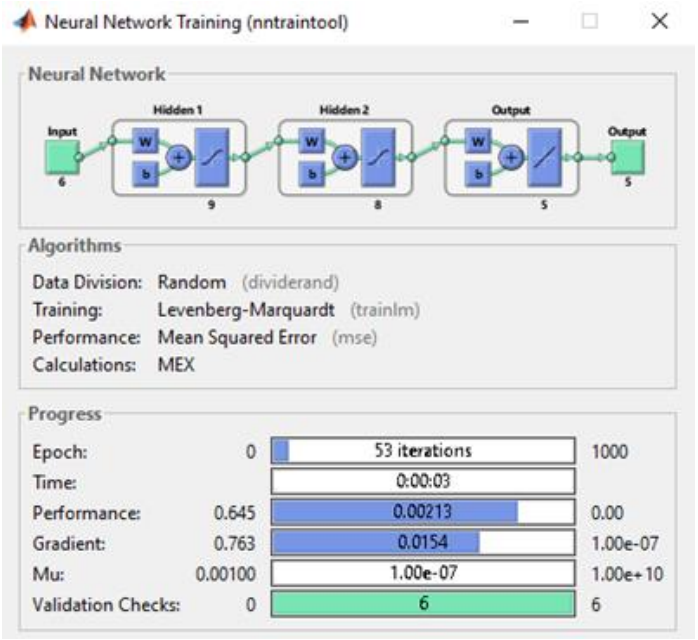

Figure 8. A screenshot of the MATLAB neural network-based fault identification method

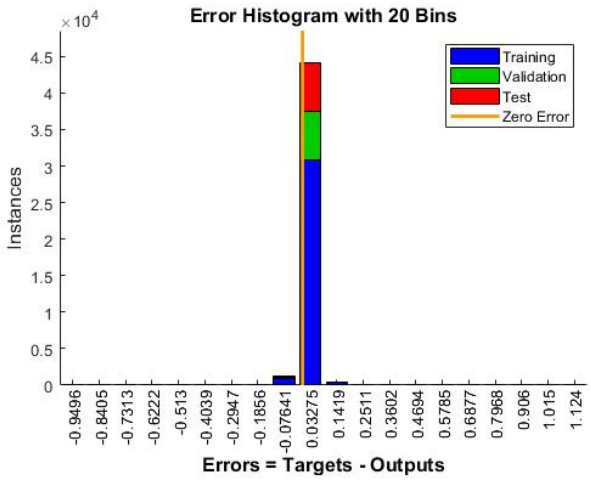

Figure 9. Error histogram of training with combined grid-connected and islanded data

IJIREEICE ISSN (O) 2321-2004, ISSN (P) 2321-5526

International Journal of Innovative Research in Electrical, Electronics, Instrumentation and Control Engineering

Impact Factor 8.021 ⁜ Peer-reviewed & Refereed journal ⁜ Vol. 12, Issue 11, November 2024

DOI: 10.17148/IJIREEICE.2024.121101

B. TESTING OF NEURAL NETWORK FAULT IDENTIFICATION METHOD

The trained neural network from the previous section is tested using trained and untrained data. Testing with trained data validates the efficacy of the training, untrained data test confirms the appropriateness of the proposed neural network method for identification of microgrid faults.

The same trained data is used to test the neural network first. This data has a total of 9,234 samples consisting of 4,788 for the grid-connected mode and 4,446 for the islanded operation mentioned in the previous section. The neural network output is near to 1 if the input currents and voltages are for that fault otherwise the output is near to 0. Figure 10 shows neural network output for a phase-to-ground fault. It can be seen, the output is near to 1 for 10 periods corresponding to 10 fault distances of grid-connected mode, and 10 periods corresponding to 10 fault distances of islanded mode. The output is near to 0 for the remaining periods. Similar results are obtained for phase-to-phase-to-ground fault, phase-to-phase fault, and three-phase fault.

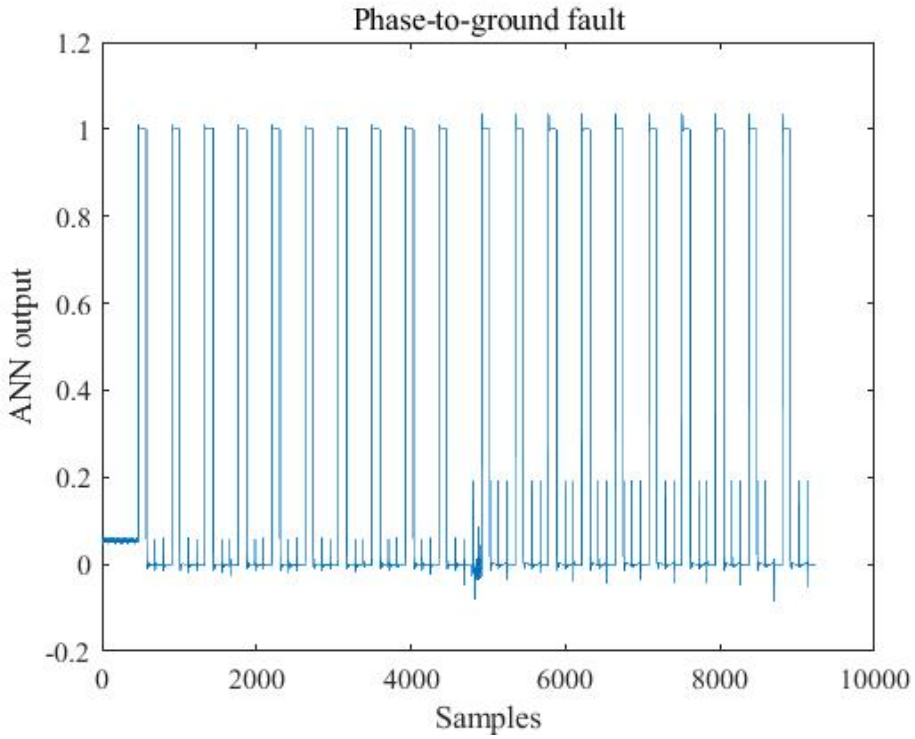

Figure 10. Neural network output for phase-to-ground fault trained grid-connected and islanded modes data

The neural network is also tested with the untrained data for four types of faults for both grid-connected and islanded modes. For the grid-connected mode, fault at 25% distance of the line from the relay location mentioned in the previous section is considered, while for the islanded mode, fault at 55% distance is considered in addition to other distances. The neural network output is near to 1 if the input currents and voltages are for that fault otherwise the output is near to 0. For phase-to-ground fault, Figure 11 shows neural network output for grid-connected data while Figure 12 shows output for islanded data. This data contains a total of 108 samples indicating three-cycles of fault for each condition. For phase-to-phase-to-ground fault, phase-to-phase fault and three-phase fault also the neural network output for grid-connected data and islanded data showed similar test results with untrained data. Table III summarizes this untrained data results of the neural network for one case of each fault and no-fault conditions. As it can be observed from this data, the neural network output is near to 1 when the RMS values of currents and voltages are for that condition otherwise it is near to 0.

As indicated before, it is expected that fault identification systems work for both grid-connected and islanded modes of operation without changing protective relay settings. Therefore, the successful identification of faults by the neural network trained with combined data in this section ascertains possibility of accomplishing this using machine learning techniques.

IJIREEICE ISSN (O) 2321-2004, ISSN (P) 2321-5526

International Journal of Innovative Research in Electrical, Electronics, Instrumentation and Control Engineering

Impact Factor 8.021 ⁜ Peer-reviewed & Refereed journal ⁜ Vol. 12, Issue 11, November 2024

DOI: 10.17148/IJIREEICE.2024.121101

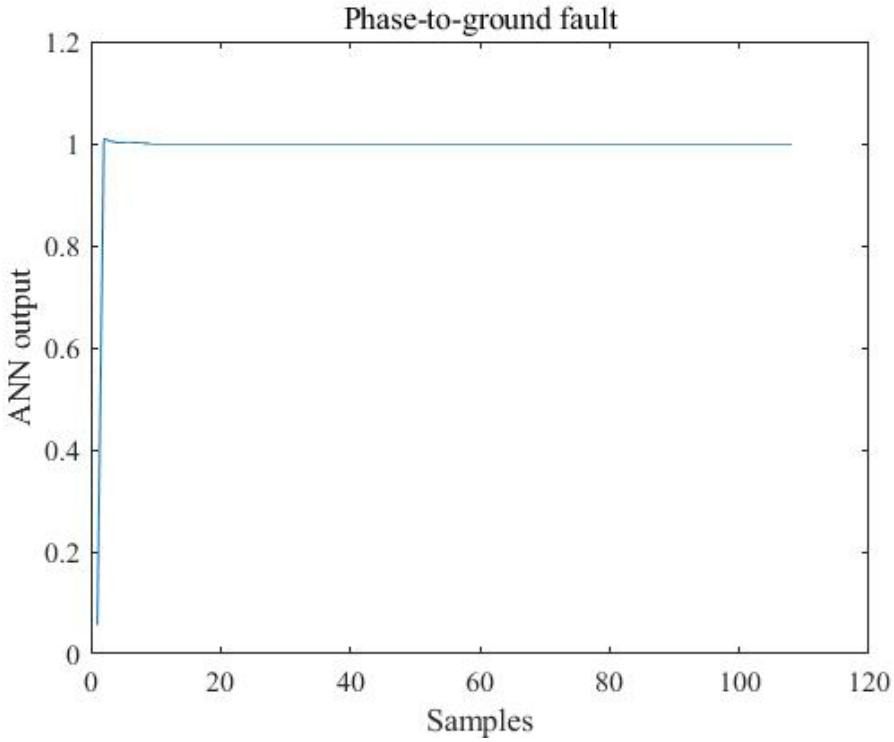

Figure 11. Neural network output for phase-to-ground fault untrained grid-connected mode data

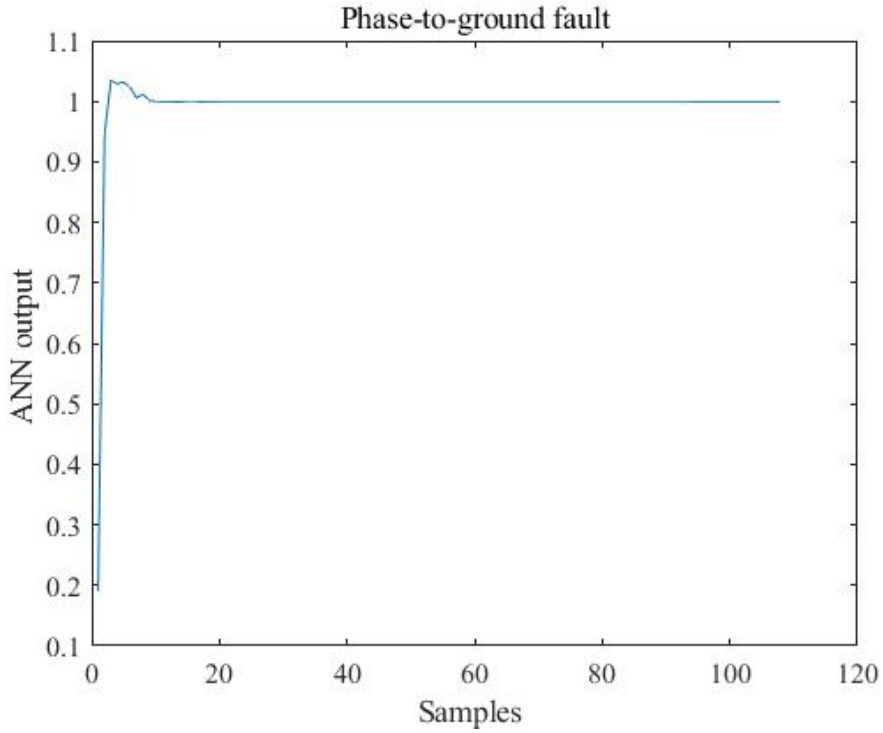

Figure 12. Neural network output for phase-to-ground fault untrained islanded mode data

DOI: 10.17148/IJIREEICE.2024.121101

Table III Input currents and voltages, and corresponding neural network outputs for grid-connected and islanded data.

Inputs						**Outputs**				
Va	Vb	Vc	Ia	Ib	Ic	NF	PG	PP	PPG	3PG
Grid-connected data										
2411.7	2466.6	2406.1	138	128	139	0.9015	0.0615	0.0245	0.0113	0.0012
358.7	2993.6	2843.8	6460	155	164	-0.0002	0.9997	0	0.0001	0.0003
2386.6	1221.1	1232	137	8280	8151	-0.0009	0.0003	1.0012	-0.0002	-0.0004
2960	306.3	351.5	170	8828	8297	0.0003	-0.0018	0.0011	1.0003	0.0001
302.7	304.6	305.9	10803	10790	9313	0.0035	-0.0027	-0.0021	0.0017	0.9995
Islanded data										
2417.5	2461.5	2388.9	391.9	438	405.7	0.9088	0.0686	0.0307	0.0696	-0.0777
174	2540.2	2759.7	1128.7	501.5	405.2	0	0.9995	0	0.0001	0.0004
2084.3	1032.8	1077.8	42.7	1176.9	1139.2	0.0014	-0.0032	1.0101	-0.0055	-0.0029
2576.2	122.1	141.3	271.8	1261.1	1288.5	-0.0034	0.0046	-0.0054	1.005	-0.0008
83.4	86.8	92.4	1341.7	1335.2	1327.9	0.0037	-0.0027	-0.002	0.0017	0.9994

V. CONCLUSION

The neural network-based machine learning technique is applied for identifying faults in a microgrid in this paper. The microgrid model used integrated renewable sources into a modified IEEE 13 node test feeder system. The simulations included four types of shunt faults at different distances and normal operation of a distribution line. Comparing the simulation of grid-connected mode of operation to islanded mode, the grid-connected mode steady-state fault currents are higher than the islanded mode. The RMS voltages and currents obtained with DFT are used to train and test the neural network. Two hidden layer neural network trained well with the microgrid data while single hidden layer network could not. The trained neural network detected four types of faults and the no-fault condition by the relay located at bus 671. It is expected that fault identification systems work for both grid-connected and islanded modes of operation without changing protective relay settings. Therefore, the successful identification of faults by the neural network trained with combined data in this paper ascertains possibility of accomplishing this using machine learning techniques.

REFERENCES

[1]. A. C. Z. de Souza and M. Castilla, Microgrids Design and Implementation: Switzerland AG: Springer Nature, 2019.
[2]. A. Hooshyar and R. Iravani, “Microgrid protection,” Proceedings of the IEEE, vol. 105, no. 7, pp1332-1353, 2017.
[3]. E. Sortomme, S. S. Venkata and J. Mitra, "Microgrid protection using communication-assisted digital relays," IEEE Transactions on Power Delivery, vol. 25, no. 4, pp. 2789-2796, 2010.
[4]. S. M. Brahma, T. Jonathan and J. Stamp, "Insight into microgrid protection," IEEE PES Innovative Smart Grid Technologies, pp. 1-6, 2014.
[5]. S. Beheshtaein, R. M. Cuzner, M. Forouzesh, M. Savaghebi and J. M. Guerrero, "DC Microgrid protection: A comprehensive review," IEEE Journal of Emerging and Selected Topics in Power Electronics, 2019, doi: 10.1109/JESTPE.2019.2904588.
[6]. Special issue on microgrid protection, IEEE Power & Energy Magazine, vol. 19, No. 3, May/June 2021.
[7]. M. W. Altaf, M. T. Arif, S. N. Islam and M. E. Haque, "Microgrid protection challenges and mitigation approaches–A comprehensive review," IEEE Access, vol. 10, pp. 38895-38922, 2022.
[8]. M. Uzair, L. Li, M. Eskandari, J. Hossain and J. G. Zhu, “Challenges, advances and future trends in AC microgrid protection: With a focus on intelligent learning methods,” Renewable and Sustainable Energy Reviews, vol. 178, 2023, 113228.
[9]. H. F. Habib, C. R. Lashway and O. A. Mohammed, "On the adaptive protection of microgrids: A review on how to mitigate cyber attacks and communication failures," IEEE Industry Applications Society Annual Meeting, 2017.

DOI: 10.17148/IJIREEICE.2024.121101

[10]. H. Lin, J. M. Guerrero, C. Jia, Z. H. Tan, J. C. V. Quintero and C. Liu, "Adaptive overcurrent protection for microgrids in extensive distribution systems," Proceedings of the IECON 42nd Annual Conference of IEEE Industrial Electronics Society, 2016.

[11]. S. Dhar, et al., "Fault detection and location of photovoltaic based DC microgrid using differential protection strategy," IEEE Trans. Smart Grid, vol. 9, pp. 4303-4312, 2018.

[12]. D. A. Gadanayak and R. K. Mallick, "Microgrid differential protection scheme using down sampling empirical mode decomposition and Teager energy operator," Electric Power Systems Research, vol. 173, pp. 173-182, 2019.

[13]. H. Al-Nasseri, et al., "A voltage based protection for micro-grids containing power electronic converters," Proc. IEEE Power Engineering Society General Meeting, p. 7, 2006.

[14]. S. Lotfi-fard, et al., "Improved overcurrent protection using symmetrical components," IEEE Trans. Power Del., vol. 22, pp. 843-850, 2007.

[15]. V. Vijayachandran and U. J. Shenoy, "New protection scheme for maintaining coordination time interval among relay pairs in micro-grid by employing centralised master controller," IET Gen. Tran. Distrb., vol. 14, pp. 234-244, 2019.

[16]. A. Hooshyar and R. Iravani, "A new directional element for microgrid protection," IEEE Transactions on Smart Grid, vol. 9, no. 6, pp. 6862-6876, 2018.

[17]. W. Huang, et al., "An impedance protection scheme for feeders of active distribution networks," IEEE Trans. Power Del., vol. 29, pp. 1591-1602, 2014.

[18]. K. A. Saleh and M. A. Allam, "Synthetic harmonic distance relaying for inverter-based islanded microgrids," IEEE Open Access Journal of Power and Energy, vol. 8, pp. 258-267, 2021.

[19]. S. R. Samantaray, et al., "Differential energy based microgrid protection against fault conditions," Proc. IEEE PES Innovative Smart Grid Technologies (ISGT), pp. 1-7, 2012.

[20]. F. C. Sampaio, et al., "A multiagent-based integrated self-healing and adaptive protection system for power distribution systems with distributed generation," Electr. Power Syst. Res.,vol. 188, p. 106525, 2020.

[21]. M. Elkhatib, et al., "Protection of renewable-dominated microgrids: challenges and potential solutions," Sandia National Lab (SNL-NM), Albuquerque, NM, 2016.

[22]. R. Bekhradian and M. Sanaye-Pasand, "A comprehensive survey on islanding detection methods of synchronous generator-based microgrids: issues, solutions and future works," in IEEE Access, vol. 10, pp. 76202-76219, 2022.

[23]. Y. Hong and M. T. A. M. Cabatac, "Fault detection, classification, and location by static switch in microgrids using wavelet transform and Taguchi-based artificial neural network," IEEE Syst. Journal, pp. 1-11, 2019.

[24]. M. Shafiullah and M. Abido, "S-transform based FFNN approach for distribution grids fault detection and classification," IEEE Access, vol. 6, pp. 8080-8088, 2018.

[25]. S. Kolla and P. Onwonga, "Identification of faults in microgrid using artificial neural networks," Proc. IEEE Green Technologies Conference (GreenTech), pp. 115-120, 2020.

[26]. M.Manohar and E. Koley, "SVM based protection scheme for microgrid," Proc. Int. Conf. on Intelligent Computing, Instrumentation and Control Technologies (ICICICT), pp. 429-432, 2017.

[27]. K.Subramaniam and M. S. Illindala, "High impedance fault detection and isolation in DC microgrids," Proc. IEEE/IAS 55th Industrial and Commercial Power Systems Technical Conference (I&CPS), pp. 1-8, 2019.

[28]. S.Ranjbar,et al. "Voltage‐based protection of microgrids using decision tree algorithms," Int. Trans. Elect. Energy Syst., vol. 30 (4), p. 12274, 2020.

[29]. S.B.A.Bukhari,R. Haider, M. S. UzZaman, Y. S. Oh, G. J. Cho and C. H. Kim, "An interval type-2 fuzzy logic based strategy for microgrid protection," Electrical Power and Energy Systems, vol. 98, pp. 209-218, 2018.

[30]. E. Casagrande, W. L. Woon, H. H. Zeineldin and N. H. Kanan, "Data mining approach to fault detection for isolated inverter-based microgrids," IET Gen. Tran. Distrb., vol. 7, no. 7, pp. 745-754, 2013.

[31]. D. P. Mishra, S. R. Samantaray and J. Geza, "A combined wavelet and data-mining based intelligent protection scheme for microgrid," IEEE Transactions on Smart Grid, vol. 7, no. 5, pp. 2295-2304, 2016.

[32]. Mathworks, available at https://www.mathworks.com/products.html, 2024.

[33]. E.M. Bashier, M. B. Khan and M. Mohammed, Machine Learning: Algorithms and Applications. New York: CRC Press, 2016.

[34]. S. R. Kolla and S. D. Altman, "Artificial neural network based fault identification scheme implementation for a three-phase induction motor," ISA Transactions, vol. 46, pp. 261-266, 2007.

[35]. W. H. Kersting, "Radial distribution test feeders," Proceedings of 2001 IEEE Power Engineering Society Winter Meeting, Columbus, OH, USA; 2001.

[36]. M. A. Fouad, M. A. Badr and M. M. Ibrahim, "Modeling of a microgrid system components using MATLAB/SIMULINK," Global Scientific Journal, vol. 5, no. 5, pp. 163-177, 2017.

[37]. A. G. Phadke and J. S. Thorp, Computer Relaying for Power Systems, West Sussex, England: John Wiley and Sons Ltd., 2009.